Development of a planar multi-body model of the human knee joint

Margarida Machado[1], Paulo Flores[1*], J.C. Pimenta Claro[1], Jorge Ambrósio[2], Miguel Silva[2], António Completo[3], Hamid M. Lankarani[4]

[1] Departamento de Engenharia Mecânica, Universidade do Minho,
Campus de Azurém, 4800-058 Guimarães, Portugal

[2] Departamento de Engenharia Mecânica, Instituto Superior Técnico,
IST/IDMEC, Av. Rovisco Pais, 1, 1049-001 Lisboa, Portugal

[3] Departamento de Engenharia Mecânica, Universidade de Aveiro,
Campus Universitário de Santiago, 3810-193 Aveiro, Portugal

[4] Department of Mechanical Engineering, Wichita State University,
Wichita, KS 67260-133 USA

Abstract

The aim of this work is to develop a dynamic model for the biological human knee joint. The model is formulated in the framework of multibody systems methodologies, as a system of two bodies, the femur and the tibia. For the purpose of describing the formulation, the relative motion of the tibia with respect to the femur is considered. Due to their higher stiffness compared to that of the articular cartilages, the femur and tibia are considered as rigid bodies. The femur and tibia cartilages are considered to be deformable structures with specific material characteristics. The rotation and gliding motions of the tibia relative to the femur can not be modeled with any conventional kinematic joint, but rather in terms of the action of the knee ligaments and potential contact between the bones. Based on medical imaging techniques, the femur and tibia profiles in the sagittal plane are extracted and used to define the interface geometric conditions for contact. When a contact is detected, a continuous non-linear contact force law is applied which calculates the contact forces developed at the interface as a function of the relative indentation between the two bodies. The four basic cruciate and collateral ligaments present in the knee are also taken into account in the proposed knee joint model, which are modeled as non-linear elastic springs. The forces produced in the ligaments, together with the contact forces, are introduced into the system's equations of motion as external forces. In addition, an external force is applied on the center of mass of the tibia, in order to actuate the system mimicking a normal gait motion. Finally, numerical results obtained from

* Corresponding author: Phone: + 352 253510220; Fax: + 351 253 516007; E-mail: pflores@dem.uminho.pt

computational simulations are used to address the assumptions and procedures adopted in this study.

Keywords: Knee joint, Ligaments, Contact, Multi-body dynamics

1. Introduction

In a broad sense, there are two main approaches to model the human body, or a sub-system of it, as a biomechanical system. These, methods are either based on the finite elements analysis [1-4], or the multibody systems methodologies [5-8]. The finite element methods provide the system's state of stress and deformation at any time, and are most accurate and versatile, but tend to be very time consuming and require high level of information on the system, which may not be accessible to the common designer, and hence remain confined to research and development. Based on simplifying premises, engineers and designers prefer to use simpler and still accurate methods, such as those based on the formulation of multibody systems. By and large, finite element models are applied in cases where localized structural deformations or soft tissues need to be described and analyzed in detail, while multibody models are usually applied in cases where gross-motions are involved and when complex interactions with the surrounding environment are expected. For instance, the gait as a gross-motion simulation is usually described using multibody systems formulations.

The study of human body motion as a multibody system is a challenging research field that has undergone enormous developments over the last years [5, 9]. Computer simulations of several human capabilities have shown to be quite useful in many research and development activities, such as: (*i*) analysis of athletic actions, to improve different sports performances and optimization of the design of sports equipment, (*ii*) ergonomic studies, to assess operating conditions for comfort and efficiency in different aspects of human body interactions with the environment; (*iii*) orthopaedics, to improve the design and analysis of prosthesis; (*iv*) occupant dynamic analysis for crashworthiness and vehicle safety related research and design; (*v*) and gait analysis, for generation of normal gait patterns and consequent diagnosis of pathologies and disabilities [10-13].
In general, most of the research works developed for simulation of human tasks is based on the assumption that the joints that constrain the relative motion of the system components are considered as ideal or perfect joints. Thus, the physical and mechanical properties of the natural human joints including the effects of friction, lubrication, and intra contact force joints are neglected. Over the last few years, a good number of studies considering the phenomena associated with real joints has been presented [14-16]. These methodologies are valid for both planar and spatial systems, and have been developed for the most general multibody systems. Consequently, in order to better understand the realistic performance of human body biomechanical systems, it is important to accurately describe the characteristics of the natural human joints, from the simple ones, such as the hip joint, to the most complex ones, such as the knee joint.

The knee joint is one of the most complex synovial joints that exist in the human body, whose main functions are: to permit the movement during the locomotion, and to allow the static

stability [17]. The mobility associated with the knee joint is indispensable to human locomotion and it helps the correct foot orientation and positioning in order to overcome the possible ground irregularities. In the knee articulation, there are three types of motion, namely, flexion, rotation and sliding of the patella [18]. The knee joint includes three functional compartments, medial, lateral and patello-femoral, which make the knee quite susceptible to injures and chronic disease, such as displacement, arthritis, ligaments rupture and menisci separation. In fact, the greatest number of human ligament injuries occurs in ligaments of the knee [19]. The knee joint is surrounded by a joint capsule with ligaments strapping the inside and outside of the joint (collateral ligaments) as well as crossing within the joint (cruciate ligaments). The two medial and collateral ligaments, MC and LC run along the sides of the knee and limit the sideways motion of the knee. The anterior cruciate ligament, ACL, connects the tibia to the femur at the center of the knee and functions to limit rotation and forward motion of the tibia. The posterior cruciate ligament, PCL, located just behind the anterior cruciate ligament limits the backward motion of the tibia. These ligaments provide stability and strength to the knee joint [20]. Overall, the knee as a self-maintaining and biologic transmission system, supports and transmits biomechanical loads between the femur, tibia and fibula. In this analogy, the ligaments represent non-rigid elements adaptable within the biological transmission system. The articular cartilages act as fixed bearing surfaces, while menisci act as mobile bearings. The function of the knee muscles, as living cellular engines in concentric contraction is to provide active forces across the joint, and in eccentric contraction act as brakes and damping systems, absorbing and dissipating loads.

Over the last decades, a number of theoretical and experimental works have been devoted to the simulation of human knee joint [21, 22]. Some of these works focus on planar systems in which only the kinematic aspects have been considered. Strasser [23] presented a knee model considered as a four-bar mechanism, in which two bars represent the cruciate ligaments, while the other bars represent the femur and tibia bones. This planar model was subsequently improved by Menschik [24] by including two curves representing the femur and tibia articular surfaces. In this model, the location of the insertion areas of the collateral ligaments was studied. Crowninshield et al. [25] presented an analytical model to study the biomechanics of the knee joint. This method is the so-called inverse method, in which the ligament forces caused by a set of translations and rotations in specific directions are determined by comparing the geometries of the initial and displaced configurations of the knee joint. Wismans et al. [17] developed a three-dimensional analytical model of the knee joint. This model considers not only the knee geometric properties, but also the static equilibrium of the system. They included a three-dimensional curved geometry of the tibia and femur surfaces, as well as nonlinear elastic spring to model ligaments. The solution method used in this approach was also a quasi-static one. Hence, in this inverse method, it is necessary to

specify the external force required for the preferred equilibrium configuration. The artificial restrictions of the quasi-static inverse method, such as the necessity to specify the preferred configuration, can be eliminated if the dynamic parameters of the problem are incorporated into the dynamic models, as it is the case presented in the present study. Moeinzadeh et al. [26] developed a two-dimensional dynamic model of the knee including ligament resistance, and specified a force and moment on the femur. A similar model was developed by Abdel-Rahman and Hefzy [27], which was later extended to three-dimensions [28]. Engin and Tumer [29] developed a two-dimensional dynamic model of the knee, which included a patella component. Blankevoort and Huiskes [30], and Mommersteeg et al. [31], developed and experimentally verified a three-dimensional knee model with surrounding soft tissue. More recently, Piazza and Delp [32] presented a rigid body dynamic model of a total knee replacement performing a step-up task. Patterns of muscle activity and kinematics of the hip were measured experimentally and used as inputs to the simulation. The model included both tibio-femoral and patello-femoral interactions and predicted the flexion-extension pattern of the step-up activity.

The dynamic modeling of the intact human knee joint is presented and analyzed in this work. The proposed model is developed under the framework of the multibody systems methodologies. The femur and tibia bones are considered as rigid bodies, and their articular cartilages are modeled as deformable elements. The shapes of the femur and tibia are obtained from magnetic resonance image technique, defined in the sagittal plane. After digitalizing the images produced, the outlines of the profiles are descritized and described in polar coordinates. A cubic interpolation spline technique approach is utilized for the profiles in order to ensure continuity in the first and second function derivatives. Thus, based on the kinematic configuration of the system, it is possible to evaluate whether the femur and tibia are in contact with each other. When a contact occurs, a continuous constitutive law is applied to the system in order to compute the contact forces produced by the contact. These resulting forces are then introduced into the system's equations of motion as external generalized forces [33-38]. These contact forces are dependent on the relative deformation between femur and tibia, as well as on the contacting surface properties, such as Young's modulus and Poisson's ratio. In addition, in the present study, the four basic ligaments that exist in the knee articulation are modeled as non-linear elastic springs. The patello-femoral and menisci are not included in the present knee model.

The main features that characterize and distinguish the model proposed here are: (*i*) the model is a dynamic one, since it relates the body forces with the motion produced, and hence it is more appropriate for studying human daily activities compared to static models [17]; (*ii*) this model explicitly relates the knee mechanical properties and the contact forces produced, what is not the case in almost all the models available in the literature [25-29]; (*iii*) the model is simple, generic

and easy to implement in other types of biomechanical systems, such as those that consider human whole-body gross motion [6]; (*iv*) the model does not contain any conventional kinematic joint and is hence capable of representing of all modes of the knee motion. Furthermore, the paper presents an important application of multiboby dynamics analysis in biomechanical modeling and analysis. In particular, a number of contributions can be cited: (*i*) the geometry definition of the femur and tibia profiles in sagittal plane from medical imaging techniques; (*ii*) the method for contact detection; (*iii*) the nature and the evaluation of contact forces using Hertzian approach models; (*iv*) and the modeling of the ligaments including the two cruciates and two collaterals. The procedure for defining surfaces and detecting contacts is rather general and could be utilized for any multibody system modeling encountering a contact-impact. The contact forces are evaluated from well-established contact force models in the literature. A continuous force approach is adopted to represent the contact interaction between femur and tibia: the corresponding rigid profiles are taken into account for contact detection and penetration calculation, while the physical properties of the articular cartilages are introduced as the contact force parameters. This issue has not been addressed before in the literature. The modeling procedure for the ligaments can also be utilized to model other biomechanical models such as the ligaments in the human cervical spine. In summary, using these procedures, a rather comprehensive model of the knee is presented in this paper. The model could be useful in understanding the forces in the knee joint during various normal and extreme activities, as well as its response to impact such as those encountered in car accidents. The results can also be utilized in the design and development of artificial knees with prostheses.

2. Knee Joint Description

A brief description of the main anatomical and physical characteristics of the intact human knee joint is presented in this section. A schematic drawing of the human knee joint involving tibio-femoral and patello-femoral pairs is represented in Figure 1. The main characteristics of this joint are the contact developed between femur and tibia and between the patella and femur, as well as the four primary ligaments [20].
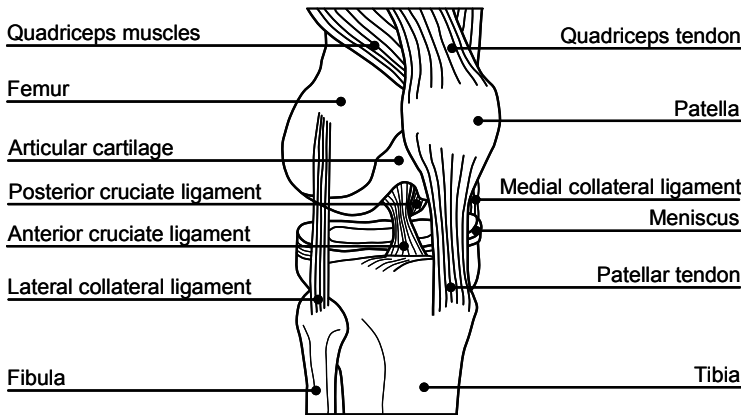

Figure 1. Representation of the intact human knee joint viewed from an anterior position [20].

The knee joint is a synovial articulation that connects the distal condylar surfaces of the femur, the proximal condylar surfaces of the tibia and the posterior surface of the patella. The primary motions of the knee are the flexion and extension on the sagittal plane. For this reason, this articulation is usually classified as a hinge joint in most studies. The flexion motion is the backward movement of the thigh or leg, while the extension motion is in the opposite direction. These motions take place about a moving transverse axis. This axis moves backward during flexion due to the curvatures of the femoral condyles. The knee flexes normally to a maximum of 135º and extends to 0º [20].

At complete flexion, the posterior femoral condylar surfaces works with the posterior tibial condylar surfaces and with the posterior portions of the menisci. During extension with the tibia fixed, the femoral condyles roll forward, while simultaneously sliding backward on the tibial condylar surfaces. Movement on the lateral condyle ends before extension is completed while movement on the medial condyle continues, since the lateral articular surface of the lateral condyle is shorter than the medial. This continued movement of the medial condyle causes the femur to rotate medially about a longitudinal axis through the lateral condyle, which ultimately taut the collateral ligaments. Thus, lateral rotation becomes a precursor to flexion. During extension, there is a lateral rotation of the tibia with respect to the femur. On a contrary, medial rotation of the tibia takes place in the beginning of flexion. When approaching complete extension, the anterior portions of the menisci are pushed forward by the femur and become less curved. The opposite effect occurs in the flexion motion. As the tibial collateral ligament becomes taut during extension, it pulls the medial meniscus outward. Figure 2 shows the main possible motions within the knee joint.
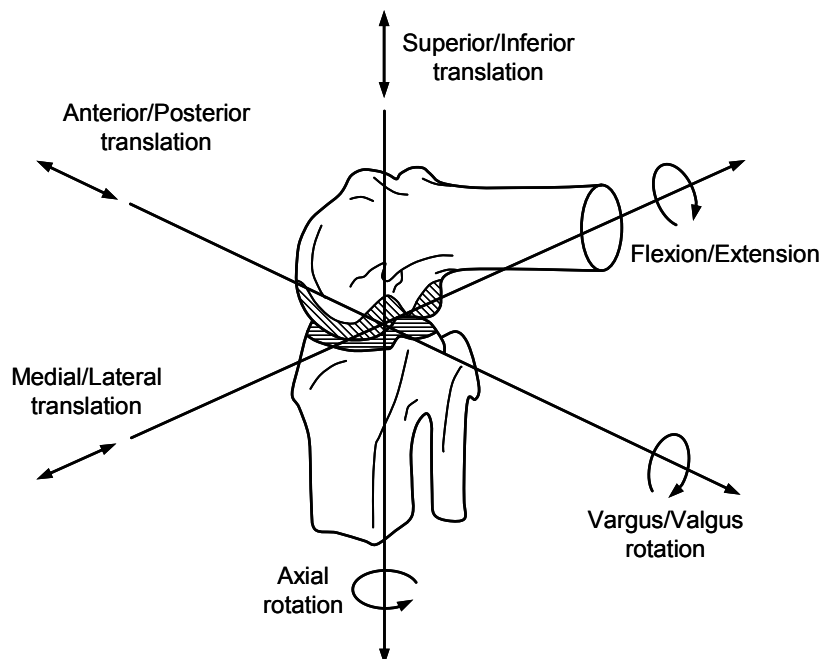

Figure 2. Six degrees of freedom of the knee that include 3 rotational and 3 translational motions.

The cruciate ligaments are taut in most positions of the knee and prevent anteroposterior displacement of the tibia in relation to the femur. During rotational movements, the cruciates twist and untwist around each other. In full flexion, the anterior cruciate ligament is relaxed and in full extension the posterior cruciate is relaxed. The collateral ligaments are relaxed when the knee is flexed to a 90º angle, thus allowing rotation about a vertical axis.

The articular surfaces of the femoral condyles are convex anteroposteriorly and form side-to-side, being more marked in the posterior portion of the anteroposterior curvature. The tibial surfaces are comparatively flat, being deepened by the wedge-shaped menisci. The patellar surface of the femur is also convex from side-to-side, with the lateral condyle extending further forward and upward.

Four major ligaments help in stabilizing the knee joint. Two of these ligaments, the anterior cruciate (AC) and posterior cruciate (PC), are located within the joint capsule. The AC is attached to the posterior side of the lateral femoral condyle and to the anterior intercondylar fossa of the tibia. The PC is attached to the anterior portion of the intercondylar notch on the femur and to the posterior intercondylar fossa of the tibia. The AC and PC touch as they span the joint with the AC passing anterior and lateral to the PC. The other two ligaments, the medial collateral (MC), also called the tibial collateral, and the lateral collateral (LC), also called the fibular collateral, are located external to the joint capsule lying medially and laterally to the joint, respectively. The AC is the primary check against anterior displacement of the tibia relative to the femur, with the PC being the primary stabilizer preventing posterior displacement. In knee flexion, the superficial MC is the first defense against external rotation with the AC acting as a secondary restraint. In knee extension, the AC and superficial MC act together as primary stabilizers against external rotation. With the knee flexed, internal rotation is prevented first by the cruciate ligaments and secondly by the LC. In extension, the AC is the primary stabilizer and the LC the secondary [39].

3. Mathematical Modeling of Knee Joint

A mathematical model for the intact human knee joint developed under the framework of multibody systems formulation is presented in this section. Figure 3 shows two bodies i and j which represent the tibia and femur, respectively. Body-fixed coordinate systems $\xi\eta$ are attached to each body, while XY coordinate frame represents the global coordinate system. The origin of the femur coordinate system is located at the intercondylar notch, while the origin of the tibia coordinate system is located at the center of mass of the tibia, with the local ξ-axes directed proximally and η-axes directed posteriorly. These origin points are represented by points O_i and O_j. The angles of rotation of the local coordinate systems of bodies i and j, relative to the global system, are denoted by ϕ_i and ϕ_j, respectively.
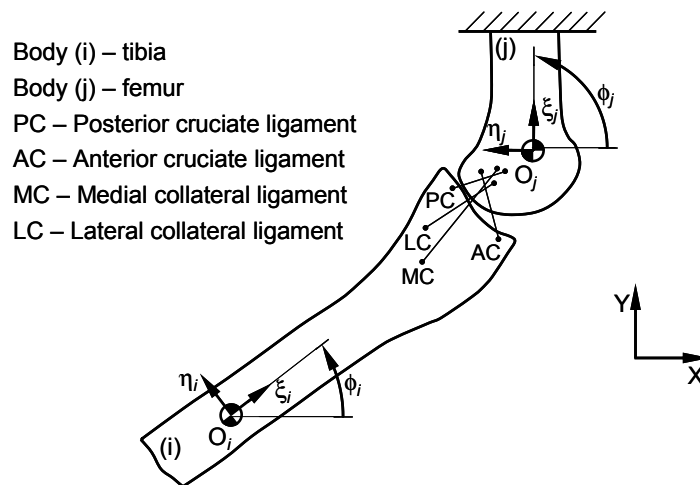
8

Figure 3. Knee joint including the femur and tibia elements and the four primary ligaments.

In the present work, the femur and tibia elements are modeled as two contacting bodies, while their dynamics is controlled by contact forces. The equations of motion that govern the dynamic response of this multibody system incorporate these contact forces. The knee joint elements are considered to be rigid and describe a general planar motion in the sagittal plane. The femur is considered to be fixed, while the tibia rolls and slides in relation to the femur profile. The femur and tibia are connected by four nonlinear elastic springs in order to represent the knee joint ligaments, as illustrated in Figure 3.

In order to develop a mathematical model for the human knee joint that allows the performance of a dynamic analysis, it is first necessary to accurately define the shapes of the femur and tibia profiles. In this work, the magnetic resonance image (MRI) technique of the knee articulation in the sagittal plane for standard size young subject population is used to obtain those profiles. Based on the MRI images, two sets of points are then considered on the articular cartilages of the femur and tibia bones. The outlines of the profiles are discretized and described in polar coordinates at the points represented in Figure 4. In order to describe these outlines in closed-form expressions, cubic spline interpolation functions are utilized, which consist of polynomial pieces on subintervals joined together according to certain smoothness conditions. For this purpose, the degree selected for the polynomial functions is 3, thus the resulting splines are cubic splines. The cubic polynomial functions are joined together in such a way that they have continuous first and second derivatives everywhere. For a complex geometry, the polynomial interpolation is generally realized by piecewise polynomial schemes. These methods construct curves that consist of polynomial pieces of the same degree and that are of a prescribed overall smoothness. The advantage of this type of interpolating procedures is that they exhibit local geometric control; i.e., the variation of the position of a control point only affects the neighborhood of that point maintaining the rest of the curve unchanged. For a detailed discussion of cubic splines interpolation, the interested reader in this issue is referred to references [40, 41].
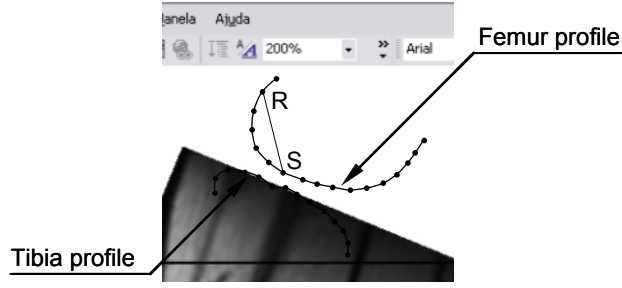
Figure 4. Magnetic resonance image (MRI) of the knee joint in the sagittal plane.

To address the femur-tibia contact interaction, it is important to develop an accurate and effective strategy to determine the location of the contact points between the profiles of the femur and tibia. The formulation proposed here requires that the profiles be convex or flat curves. An outline is convex if the straight line between any pair of points on the curve lies inside the body, such as points R and S on the femur in Figure 4.

Figure 5 shows the general configuration of a portion of the femur and tibia contacting curves, in which the relative distance between them is exaggerated to represent all the necessary vectors for the model presented. Let the contact points on bodies i and j be represented by P_i and P_j, respectively. Furthermore, it is considered that the segment of curve between points A and B on bodies i and j are defined by two cubic spline functions s_i and s_j as,

$$s_i = a_3\theta_i^3 + a_2\theta_i^2 + a_1\theta_i + a_0 \tag{1}$$
$$s_j = b_3\theta_j^3 + b_2\theta_j^2 + b_1\theta_j + b_0 \tag{2}$$

where a_0, a_1, a_2, a_3, b_0, b_1, b_2 and b_3 are the cubic spline polynomial coefficients and θ_i and θ_j represent the profile curve polar parameters that define the splines employed [41]. For describing the shape or the outline of a body, appropriate types of piecewise spline is the Akima spline and the shape preserving spline. These types of piecewise splines are designed so that the shape of the curve matches the shape of the data. The Akima spline attempts to minimize oscillations and the shape preserving spline preserves the convexity of the data [42]. It should be mentioned that these angles are measured relative to the local ξ-axis, as shown in Figure 5.

The first derivatives of Equations (1) and (2) with respect to angles θ_i and θ_j are, respectively,

$$\dot{s}_i = 3a_3\theta_i^2 + 2a_2\theta_i + a_1 \tag{3}$$
$$\dot{s}_j = 3b_3\theta_j^2 + 2b_2\theta_j + b_1 \tag{4}$$

In a similar way, the second derivatives of Equations (1) and (2) yield,

$$\ddot{s}_i = 6a_3\theta_i + 2a_2 \tag{5}$$
$$\ddot{s}_j = 6b_3\theta_j + 2b_2 \tag{6}$$

Thus, with this approach it is ensured that polynomial functions used to define the femur and tibia profiles are continuous for each interval considered.

Figure 5. Two contacting bodies, in which the distance between them is strongly exaggerated with the purpose to represent all the desired vectors.

The contact detection between freeform profiles consists of a two-step procedure. The first problem that arises is the accurate prediction of the location of the contact candidate points. The second step consists of calculating the distance between the candidate points and evaluating a penetration condition in order to check whether the points are, in fact, in contact or not [43]. Figure 5 schematically shows two bodies in contact, which could be femur and tibia. The curves s_i and s_j represent the contact profiles of bodies i and j, respectively, and the points P_i and P_j belong to curves s_i and s_j, and have potential contact points. The local coordinates of potential contact points P_i and P_j are determined in terms of the polar coordinates as [33],

$$\xi_k^P = s_k \cos\theta_k \quad (k=i,j) \tag{7}$$

$$\eta_k^P = s_k \sin\theta_k \quad (k=i,j) \tag{8}$$

The global position of the potential contact points, $\mathbf{r}_k^P$ can be expressed as,

$$\mathbf{r}_k^P = \mathbf{r}_k + \mathbf{A}_k \mathbf{s}_k'^P \quad (k=i,j) \tag{9}$$

where $\mathbf{r}_i$ and $\mathbf{r}_j$ are the global coordinates of points O_i and O_j, respectively, while $\mathbf{s}_i'^P$ and $\mathbf{s}_j'^P$ are the local components of points P_i and P_j with respect to $\xi\eta$ coordinate system. The rotational transformation matrices $\mathbf{A}_k$ are,

$$\mathbf{A}_k = \begin{bmatrix} \cos\phi_k & -\sin\phi_k \\ \sin\phi_k & \cos\phi_k \end{bmatrix} \quad (k=i,j) \tag{10}$$

The velocities of the contact points P_i and P_j expressed in terms of the global coordinate system are evaluated by differentiating Equation (9) with respect to time, yielding,

$$\dot{\mathbf{r}}_k^P = \dot{\mathbf{r}}_k + \dot{\mathbf{A}}_k \mathbf{s}_k'^P \quad (k=i,j) \tag{11}$$

in which the dot denotes the derivative with respect to time.

11

The relative normal and tangential velocities are determined by projecting the relative contact velocities onto the respective directions,

$$v_N = \left(\dot{\mathbf{r}}_i^P - \dot{\mathbf{r}}_j^P\right)^T \mathbf{n} \tag{12}$$

$$v_T = \left(\dot{\mathbf{r}}_i^P - \dot{\mathbf{r}}_j^P\right)^T \mathbf{t} \tag{13}$$

where $\mathbf{n}$ is the normal vector to the direction of contact, and $\mathbf{t}$ is the tangential vector, obtained by rotating vector $\mathbf{n}$ by 90° clockwise direction, as shown in Figure 5. Since the contacting bodies have been defined by polynomial functions, the first problem that arises is the accurate prediction of the location of the contact points. This problem has to be solved at every time step during the dynamic analysis.

From Figure 5, it can be observed that the distance between the potential contact points on bodies i and j, P_i and P_j, is given by vector $\mathbf{d}$, which can be written as,

$$\mathbf{d} = \mathbf{r}_i^P - \mathbf{r}_j^P \tag{14}$$

or,

$$\mathbf{d} = \mathbf{r}_i + \mathbf{A}_i \mathbf{s}_i'^P - \mathbf{r}_j - \mathbf{A}_j \mathbf{s}_j'^P \tag{15}$$

The first geometric condition for contact between points P_i and P_j is that the vector $\mathbf{d}$ corresponds to the minimum distance. Another geometric contact condition is that the vector $\mathbf{d}$ and normal vectors of the curves, $\mathbf{n}_i$ and $\mathbf{n}_j$, have to be collinear.

The first derivatives of Equations (7) and (8), which correspond to the local coordinates of potential contact points, with respect to θ_i and θ_j give the local components of the vectors tangent to the curves s_i and s_j at points P_i and P_j respectively, as illustrated in Figure 5. Therefore, these tangent vectors can be expressed in local coordinates as,

$$\mathbf{t}_i'^P = \left[\dfrac{d\xi_i^P}{d\theta_i} \quad \dfrac{d\eta_i^P}{d\theta_i} \right]^T \tag{16}$$

$$\mathbf{t}_j'^P = \left[\dfrac{d\xi_j^P}{d\theta_j} \quad \dfrac{d\eta_j^P}{d\theta_j} \right]^T \tag{17}$$

For points P_i and P_j, the normal vectors can be expressed in local coordinates as,

$$\mathbf{n}_i'^P = \left[\dfrac{d\eta_i^P}{d\theta_i} \quad -\dfrac{d\xi_i^P}{d\theta_i} \right]^T \tag{18}$$

$$\mathbf{n}_j'^P = \left[\dfrac{d\eta_j^P}{d\theta_j} \quad -\dfrac{d\xi_j^P}{d\theta_j} \right]^T \tag{19}$$

The tangent and normal vectors can then be easily expressed in the global form by multiplying the local coordinates, given by Equations (16)-(19), by the respective rotational transformation matrix, given by Equation (10).

The minimum distance condition given by Equation (14) is not enough to find the possible contact points between the two contact profiles, since it does not cover all possible scenarios that may occur in the contact problem. Therefore, the contact points are defined as those that correspond to maximum penetration; i.e., the points of maximum elastic deformation, measured along the normal direction [43]. The geometric condition equations for contact are defined as,

    (i)   The distance between the potential contact points, P_i and P_j, given by vector **d** corresponds to the minimum distance;

    (ii)   The vector **d** has to be collinear with the normal vector $\mathbf{n}_i$;

    (iii)   The normal vectors $\mathbf{n}_i$ and $\mathbf{n}_j$ at the potential contact points, P_i and P_j, have to be collinear, which means that $\mathbf{n}_j$ has null projection onto the tangent vector $\mathbf{t}_i$.

Conditions *(ii)* and *(iii)* can be written as,

$$\mathbf{n}_j \times \mathbf{n}_i = \mathbf{0} \quad \text{or} \quad \mathbf{n}_j^T \mathbf{t}_i = 0 \tag{20}$$

$$\mathbf{d} \times \mathbf{n}_i = \mathbf{0} \quad \text{or} \quad \mathbf{d}^T \mathbf{t}_i = 0 \tag{21}$$

The geometric conditions given by Equations (20) and (21) are two nonlinear equations with two unknowns, the two profile curve parameters θ_i and θ_j, which can be solved using a Newton-Raphson iterative procedure with Jacobians obtained by finite differences. This system of equations provides the solutions for the location of the potential contact points. Once the potential contact points are found, the next step is the evaluation of the pseudo-penetration given by,

$$\delta = d = \sqrt{\mathbf{d}^T \mathbf{d}} \tag{22}$$

The penetration condition states that the contact between body's profiles exists and, therefore, the potential contact points are real contact points when the following relation is verified,

$$\mathbf{d}^T \mathbf{n}_j \leq 0 \tag{23}$$

By introducing the curve parameters that describe the geometry of the contact profiles, the components of the contact points can be predicted during the dynamic analysis. Since the profiles of the bodies have complex geometries, the position of the contact points can not be predicted. Therefore, during dynamic simulations, the calculation of the curve parameters requires the solution of a preliminary system of nonlinear equations. The computational implementation of this methodology is quite efficient since the information of the previous time step is used as initial guess or estimate to find the solution of the nonlinear equations (20) and (21).

4. Modeling the Contact Forces

The elastic force developed in the contact between the femur and tibia can be modeled by applying a Hertzian-type contact law, which is can be expressed as [44],

$$F_N = K\delta^n \qquad\qquad (24)$$

in which F_N is the normal contact force, K is a generalized stiffness parameter and δ is the relative penetration depth, given by Equation (22). The exponent n is equal to 1.5. The generalized stiffness depends on the material properties and on the geometry of the contacting bodies. For two spheres in contact the generalized stiffness coefficient is function of the radii of the spheres i and j and the material properties as [45],

$$K = \frac{4}{3(\sigma_i + \sigma_j)}\sqrt{\frac{R_i R_j}{R_i + R_j}} \qquad\qquad (25)$$

where R_i and R_j are the radii of the spheres and σ_i and σ_j are given by,

$$\sigma_k = \frac{1 - \nu_k^2}{E_k} \quad (k = i,j) \qquad\qquad (26)$$

and the quantities ν_k and E_k are the Poisson's ratio and the Young's modulus associated with each sphere, respectively.

The Hertz contact law given by Equation (24) is a purely elastic model, and it does not include any energy dissipation. Lankarani and Nikravesh [46] extended the Hertz contact law to include energy loss due to internal damping as,

$$F_N = K\delta^n \left[1 + \frac{3(1 - c_r^2)}{4}\frac{\dot{\delta}}{\dot{\delta}^{(-)}} \right] \qquad\qquad (27)$$

where the generalized parameter K is evaluated by Equations (25) and (26) for sphere to sphere contact, or by similar expressions for the contact of other types of geometries, c_r is the restitution coefficient, $\dot{\delta}$ is the relative normal penetration velocity and $\dot{\delta}^{(-)}$ is the initial relative normal contact-impact velocity where contact is detected.

In order for the generalized stiffness parameter K to be evaluated, it is necessary to know the radii of curvature of the femur and tibia surfaces. For this purpose, the data presented by Koo and Andriacchi [47] were used, which addressed the influence of global functional loads and local contact anatomy on the articular thickness of the knee joint. Based on bilateral knee MRI images obtained from 11 young healthy adults with no history of knee injury, Koo and Andriacchi observed a consistent pattern among the individuals at the thickest regions of the contact surfaces. The femur cartilage presents convex curvatures in both medial and lateral compartments. The tibia cartilage has concave curvatures for medial compartments and convex curvature for the lateral compartment. Figure 6 shows the average radii of the curvatures in both lateral and medial compartments [47], where the values are expressed in millimeters. Moeinzadeh et al. [26] and Abdel-Rohmam and Hefzy [27] used similar values for the radii of curvature for the medial compartment only. It should be noted that in general, the applied load is higher in the lateral compared to medial compartments,

since the articular cartilage is thicker in the lateral than medial compartments. This is logical as the contact surfaces conformed best (convex-concave surfaces) in the medial compartment, and worst (convex-convex surfaces) in the lateral compartment.
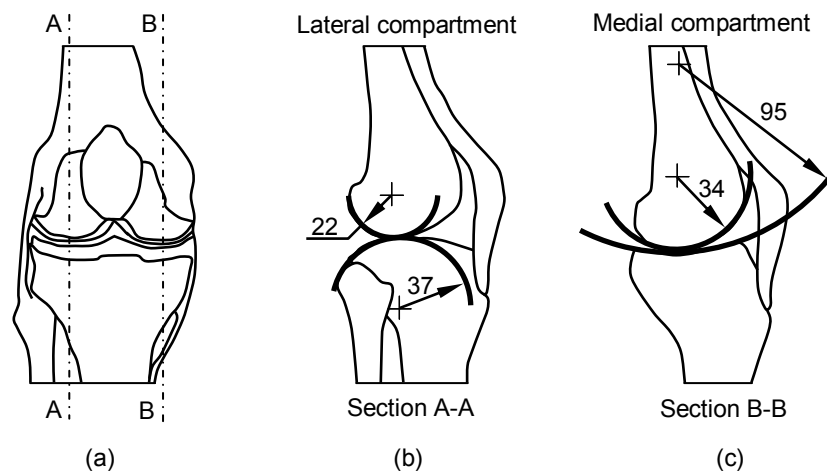

Figure 6. Average radii in millimeters of the femur and tibia articular cartilages: (a) Coronal view; (b) Lateral compartment; (c) Medial compartment [47].

5. Physical Models for the Ligaments and Capsule

It is known that ligaments are composite and anisotropic structures exhibiting nonlinear time and history dependent viscoelastic properties. The time dependent response means that, during daily activities, ligaments are subjected to a variety of load conditions that influence their physical properties. Thus, for example, ligaments become softer and less resistant after some minutes of running, returning to normal hardness when the exercise is interrupted. The history dependence, in turn, means that frequent intense activities changes the tissue properties in a medium term basis. For example, the ligaments of an athlete, after 6 months of daily training, become softer and thus more adapted to the intense exercise, even when the athlete is not training. In the same way, if the activities are interrupted for some months, the ligament properties go back to normal levels. Ligaments are also temperature and age sensitive [19].

A typical stress-strain relationship for a general ligament is illustrated in Figure 7, in which three different zones can be identified [48]. These zones can be analyzed and understood in terms of microarchitecture of ligament. Zone I corresponds to the geometrical rearrangement of microstructural network, that is, uncoiling of the coiled collagen fibers. In this zone, the ligament stiffness is determined mainly by the stiffness of the elastin network. The stiffness increases since the fibers become aligned. In this zone, the ligaments elongate with forces that act on them. At the end of the zone I, all collageneous fibers are assumed to be fully uncoiled. In zone II, the stiffness of ligaments is reported to correspond mainly to the stiffness of the collagen fibers and is found to be almost constant. Finally, in zone III, the rupture of some collagen fibers is observed, followed by a complete failure of the ligament itself [21, 22].
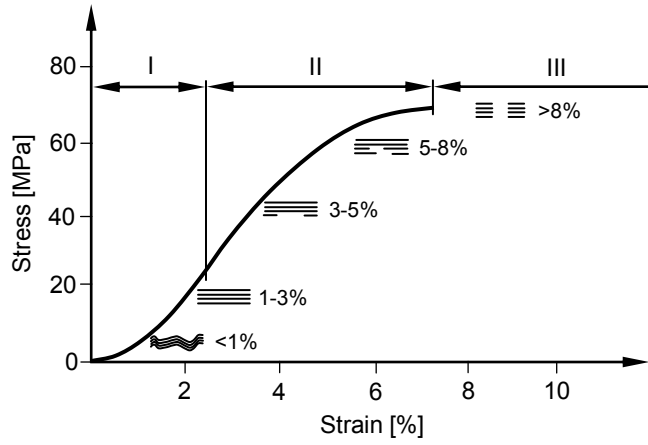
Figure 7. Typical ligament stress-strain relationship [48].

Based on the information given by stress-strain curve of Figure 7, the force-elongation relationship can be represented by a quadratic equation. Crowninshield et al. [25] tested human knee ligaments and observed that a quadratic stress-strain function is a good approximation for the elastic behavior of the ligaments. In the present study, the following force-elongation relation is considered for each knee ligament [26-29],

$$F_l = k_l \left(l_l - l_l^0 \right)^2, \quad if \quad l_l > l_l^0 \tag{28}$$

where, k_l is the ligament stiffness, l_l and l_l^0 are the current and initial or undeformed lengths of the ligament, respectively. Furthermore, it is assumed that ligaments can not carry any compressive force; that is,

$$F_l = 0, \quad if \quad l_l \leq l_l^0 \tag{29}$$

The direction of the force exerted by ligament on the articulating body coincides with the direction of the line segment through the insertion points of the ligaments. These insertion points represent the end points of the ligaments and are connected to the femur and tibia articular surfaces. The distance between the insertion points defines the length of the ligament. The location and stiffness of the ligaments will be presented in the next section.

In this study, the bone portions of the distal femur and proximal tibia are considered as perfectly rigid, due to their much higher stiffness when compared to the significant soft tissues. The articular cartilages are modeled as deformable material. Articular cartilages are composed of a solid matrix, which consists of protoglycans, collagens and water. Articular cartilages are structurally non-homogeneous and possess anisotropic and nonlinear mechanical behavior. Yet, for sake of simplicity, most analytical models consider articular cartilages homogeneous and isotropic material [49]. The most important physical properties of the articular cartilages are the elastic Young's modulus, Poisson's ratio and the permeability. The study of cartilage performance is of paramount importance because the damage in cartilage is a problem that affects millions of people in the world. Causes for damage in cartilages are osteoarthrosis, osteochondrosis and trauma [50, 51].

16

6. Results and Discussion

In this section, some numerical results obtained from computational simulations of the developed model are presented and discussed in order to understand the dynamic behavior of the knee joint model proposed in this work. Figure 8 shows the initial configuration of the multibody model of the intact human knee joint, which consists of two rigid bodies representing the femur and tibia. The femur is fixed, while the tibia is considered to move relative to the femur. The acceleration due to gravity is taken as acting in the negative *Y*-direction and the system is defined as moving in a vertical plane, corresponding to the motion described in the sagittal plane. The Cartesian coordinates of centers of mass and inertia properties of the femur and tibia are listed in Table 1, which are assigned to the segments on values derived for a similar model of a 76 kg, 1.8 m tall male by Yamaguchi [52].
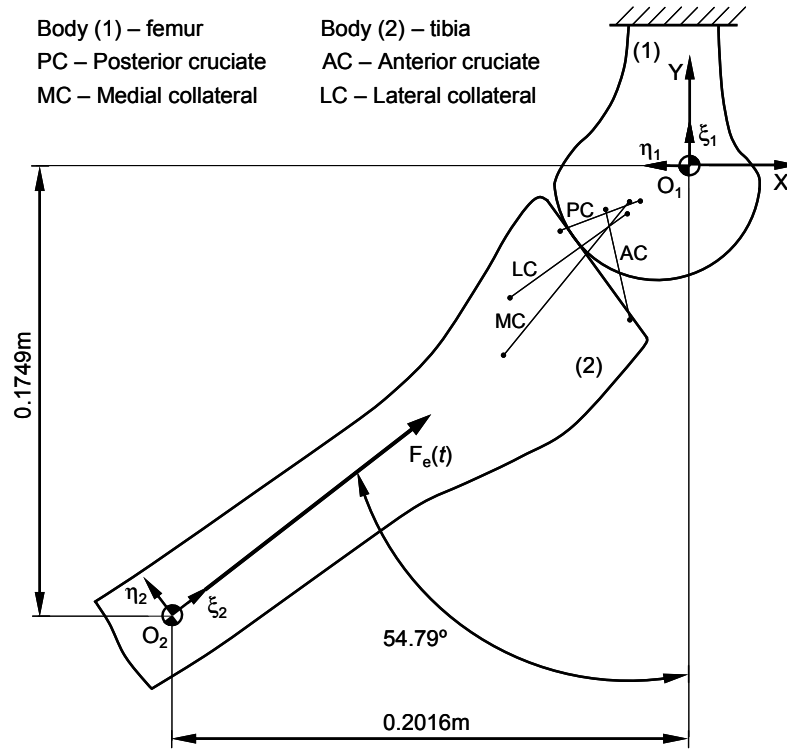
Figure 8. Initial configuration of the multibody intact human knee join model.

Body name	x [m]	y [m]	ϕ [°]	Mass [kg]	Moment of inertia [kgm^2]
Femur	0.0000	0.0000	90.00	7.580	0.126
Tibia	-0.2016	-0.1749	35.21	3.750	0.165

Table 1. Cartesian coordinates and inertia properties of the femur and tibia bodies [52].

The four basic ligaments present in the knee articulation, the two cruciates and the two collaterals, are modeled as nonlinear elastic springs elements. All ligaments carry force if their current lengths are longer than their initial lengths. The initial lengths were determined when femur and tibia are positioned at 54.79 degrees of knee flexion, since this value corresponds to a particular position where the ligaments are in a relatively relaxed condition, as examined by Moeinzadeh [22].

The local coordinates of the ligament insertion points, as well as the physical ligament properties, such as stiffness (k_l), maximum allowable strains (ε) and forces (F_l), are summarized in Table 2. These values are determined from the available information in literature and close to anatomical study of human knee joint [21, 29].

Ligament	ξ_1^l [m]	η_1^l [m]	ξ_2^l [m]	η_2^l [m]	l_0 [m]	k_l [N/m^2]	ε [%]	F_l [N]
ML – Medial collateral	-0.023	-0.014	0.163	0.008	0.0784	15×10^6	17	534
LC – Lateral collateral	-0.025	-0.019	0.178	0.025	0.0562	15×10^6	-	-
AC – Anterior cruciate	-0.033	-0.017	0.213	-0.009	0.0438	35×10^6	22	622
PC – Posterior cruciate	-0.019	-0.014	0.210	0.035	0.0332	30×10^6	19	868

Table 2. Local coordinates of the insertion points of the ligaments and physical ligament properties [21, 29].

The articular cartilages of the knee are modeled as linear elastic and isotropic material with an elastic modulus of E=5 MPa and a Poisson's ratio of v=0.46 [53]. This can be considered accurate enough to predict cartilage response, as demonstrated by Donzelli et al. [54]. In addition, in the present work, and for sake of simplicity, the tibia is considered to be a planar surface, and the femur cartilage is modeled as a curved surface with radius equal to 0.04 m [47]. Table 3 shows the dynamic parameters used in the computational simulations.

Cartilage Young's modulus	5 MPa
Cartilage Poisson's ratio	0.46
Cartilage restitution coefficient	0.30
Cartilage friction coefficient	0.00
Integration step time	0.00001s
Integration tolerance	0.000001

Table 3. Parameters used in the dynamic simulation of the knee joint model.

In the dynamic simulation, the knee joint model is released from 54.79 degrees of knee flexion. Besides the gravitational force, an external force, typical of the load encountered during a normal gait ground reaction, is applied at the centre of mass of tibia directed proximally, as illustrated in Figure 8. The external force is located directed proximally, since it corresponds to a resultant force of a horizontal component, which provides the tibia motion at the sagittal plane from a posterior position to an anterior one, and a vertical component force, which ensures that the tibia slides along the femur profile. The aim of this force is so to provide a dynamic action to the knee joint model; i.e., to induce the tibia motion from a flexion position at 54.79º to an extension position at 0º. The hyperextension scenario has not been taken into account in the computational simulations, although it's important to mention that, in general, 1 to 3 degrees of hyperextension is anatomically tolerable, beyond which joint failure becomes unavoidable. The external applied force, F_e, is expressed as,

$$F_e = Ae^{-4.73\left(\frac{t}{t_d}\right)^2} \sin\left(\frac{\pi t}{t_d}\right) \tag{30}$$

which is an exponentially decaying sinusoidal pulsed function of duration t_d and with an amplitude A. The external force defined by Equation (30) was selected with the fundamental purpose of validating the developed methodology. This exponentially decaying sinusoidal pulse function was selected as it represents the dynamic behavior in daily human activities; i.e. the forces applied on the anatomic segments vary both in magnitude and direction. This same type of applied external force has been used in computational simulations of other biomechanical models, such as in modeling and simulation of the quadriceps muscle force in knee extension and of human head neck studies [26, 55]. In the present study, the influence of pulse duration on the dynamic response of the knee joint motion is not considered. A pulse duration of 0.05 s is selected in this study. However, two different values of the pulse amplitude A are considered in the computational simulations, in order to evaluate the influence of the force magnitude on the knee joint contact dynamics.

Computational simulations were performed to study first how the type of cubic spline interpolation used to define the geometry of the contact profiles influences the knee dynamic behavior. To interpolate the set of points extracted by manual segmentation from a MRI image, three different interpolation techniques; namely cubic splines, Akima splines and shape preserving splines were utilized [41]. For the three cases, the computational simulations were carried out based on the methodology of contact detection presented in Section 3 and considering an external applied force with amplitude equal to 50 N. The Hertzian-type contact law was used to model the contact force. Figure 9 shows the coordinates of the tibia contact points and the relative deformation obtained for each simulation.
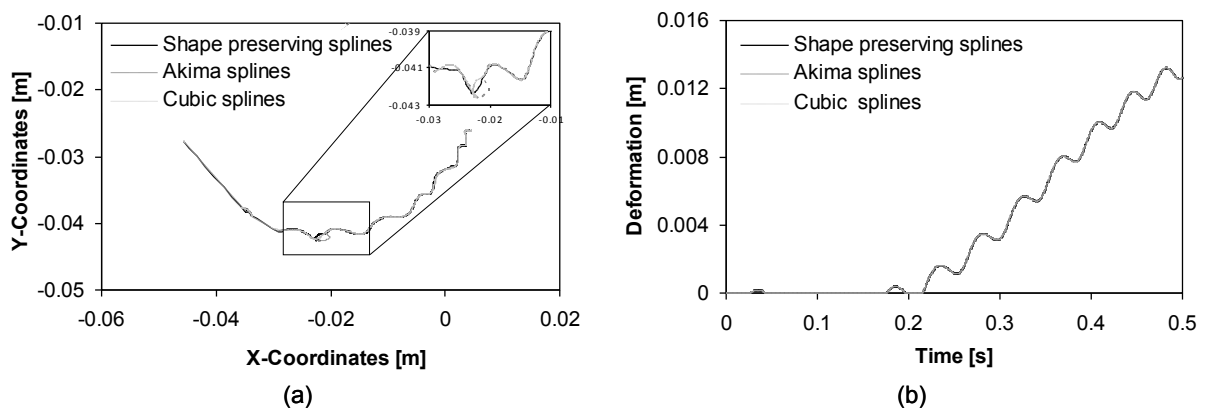

Figure 9. (a) Tibia contact points; (b) Local deformation/indentation.

From Figure 9, it can be observed that the choice for the cubic interpolation spline technique does not have significant influence on the resulting motion. However, it is possible that such differences occur when the profile geometries are more complex. For a generic methodology, the shape preserving interpolation splines is elected as cubic interpolation technique. According to Pombo and Ambrósio [56], this type of cubic interpolation is more appropriate for defining the shape of the

body outlines compared with other interpolating curves, such as cubic splines and Akima splines, since they do not introduce spurious oscillations on the curves.

The second series of computational simulations was to study the knee contact dynamic response based on different contact force models. The simulations were carried out using the pure Hertzian contact law and the Lankarani and Nikravesh force model, and the results were compared as illustrated in plots of Figures 10 and 11. This procedure was performed taking into account the methodology of contact detection presented in Section 3 and considering an external force with amplitude equal to 50 N. To define the contacting surface profiles, shape preserving interpolation splines were utilized.

(a)   (b)
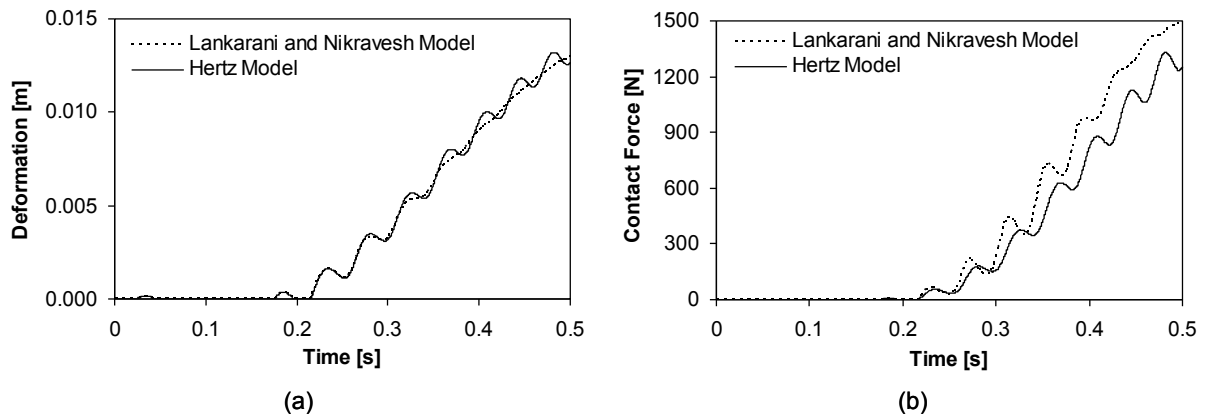
Figure 10. (a) Local deformation/indentation; (b) Normal contact force.

(a)   (b)
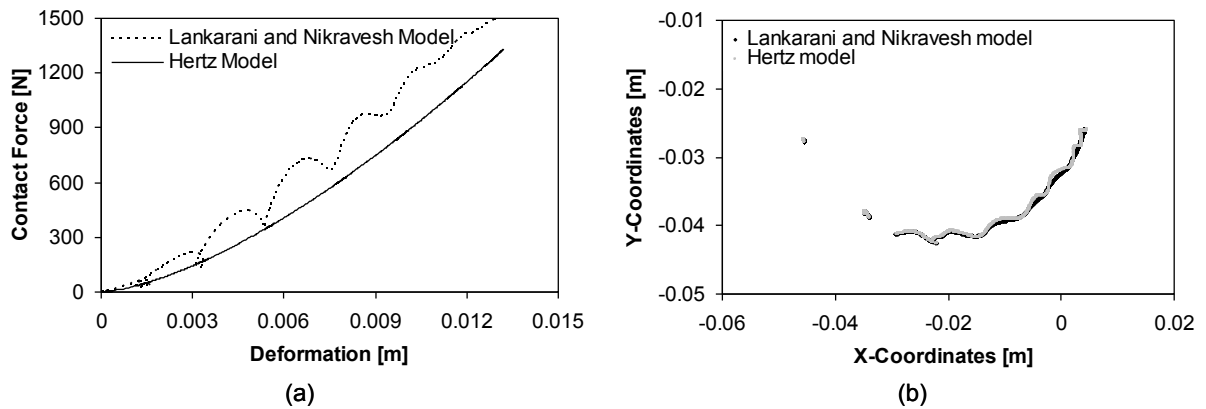
Figure 11. (a) Normal contact force versus deformation; (b) Tibia contact points.

For the Hertz contact law, Figures 10(a) and 10(b) depict that the deformation and normal contact force have curves with similar shapes. This is a congruent result since the Hertz model does not take into account the energy dissipation during impact, which strongly depends on impact velocities. Figure 11(a) shows that the contact energy stored during the loading phase is exactly the same as that restored during the unloading phase. For the Lankarani and Nikravesh model, Figure 10(a) shows a deformation similar to the Hertz model. The normal contact force, plotted in Figure 10(b), exhibits some differences since the Lankarani and Nikravesh model takes into account the energy loss during impact. Figure 11(a) confirms the existence of energy dissipation since the

corresponding curve for Lankarani and Nikravesh model represents a non-injective function, which means that the hysteresis factor of the Equation (27) is not null. The curve shape suggests that there are contacts with two phases, a complete loading phase and an incomplete unloading phase. The interruption of the unloading phase happens because another contact; i.e., another loading phase occurs. This phenomenon can explain the smaller hysteresis loops present in Figure 11(a) for the Lankarani and Nikravesh model. Figure 11(b) shows some minimal differences in tibia contact points trajectory, which are associated with the energy dissipation accounted by Lankarani and Nikravesh model.

In order to study the influence of the amplitude of external applied force on the knee contact dynamics, simulations with different amplitudes for the external applied force were performed. These computational simulations are based on the methodology of contact detection presented in Section 3 and considering a pure Hertzian contact. Moreover, the shape preserving interpolation technique defines the contact profiles. Figure 12 shows the tibia centre of mass coordinates and the knee flexion angle as function of time for amplitudes of external applied force equal to 50 N and 150 N. Figures 13 and 14 illustrate the dynamic results of the nonlinear elastic springs, which represent the knee ligaments, for external applied forces of 50 N and 150 N. Figure 15 shows the coordinates of the tibia contact points and the relative deformation obtained for each situation. From Figures 12(a) and 12(b), it can be observed that the amplitude of the external applied force does not have a significantly influence on the position of tibia centre of mass and the knee flexion angle, since these parameters are practically the same for both values of amplitude. In sharp contrast, for the dynamic response of the knee ligaments some differences are observed. In fact, the increase of the amplitude of the externally applied force increases the ligament strains and the ligament forces, as observed by comparing Figures 13 and 14. This rise occurs as the ligaments act as the only force element present in the knee joint, and hence, are the only elements that restrict the tibia movement. For the amplitude of the external applied force equal to 50 N, the results indicate that when the knee extends in response to the applied forces on tibia, medial collateral ligament (MCL) and lateral collateral ligament (LCL) strains and forces are lower than those for the anterior cruciate ligament (ACL) and posterior cruciate ligament (PCL). This confirms the fact that the cruciate ligaments are commonly injured, especially during sport activities and motor vehicle accidents [57]. The small resistance of the MCL and LCL, visible in Figures 13 and 14, is evident since the main role of these two ligaments is to offer varus-valgus and internal-external rotational stability [18]. For the amplitude of the external applied force equal to 150 N, some of the physiological ligament behaviors reported for an amplitude equal to 50 N were not verified. This occurs because when the amplitude of the external force increases, the contact forces increases also and these high contact forces affect the dynamic response of the ligaments. As it can be observed

from Figure 15(b), for an amplitude of the external applied force equal to 150 N, the results of the tibia contact points represents a non-physiological scenario, since the human body does not tolerate these loading situations without damage or injuries on biological tissues surrounding the knee.
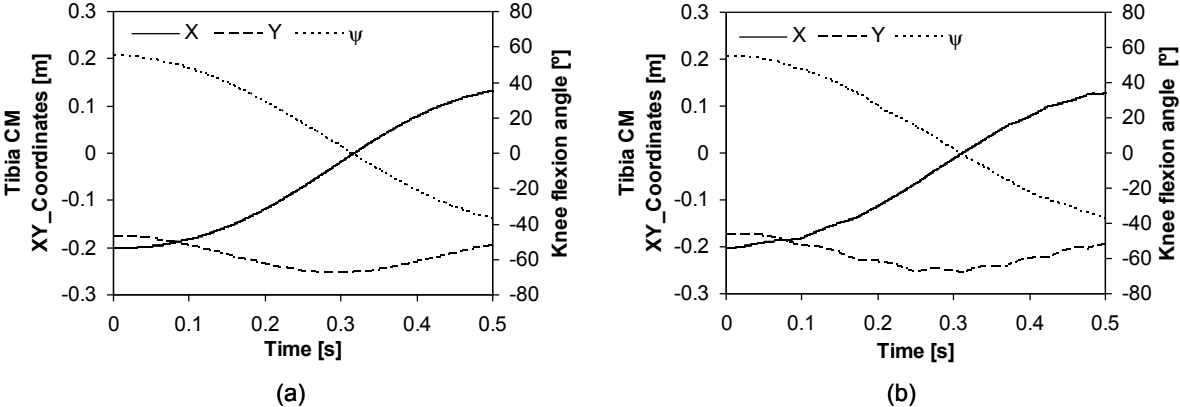

(a)

(b)

Figure 12. Tibia centre of mass coordinates and knee flexion angle for an amplitude of external applied force equal to: (a) 50 N and (b) 150 N.
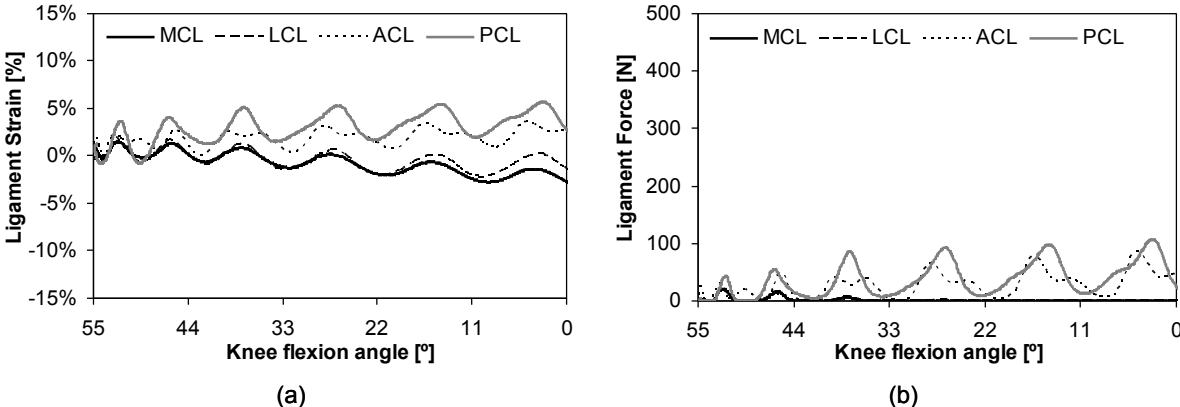

(a)

(b)

Figure 13. (a) Ligament Strain versus Knee flexion angle for an amplitude of external applied force equal to 50 N; (b) Ligament Force versus Knee flexion angle for an amplitude of external applied force equal to 50 N.

(a)

(b)
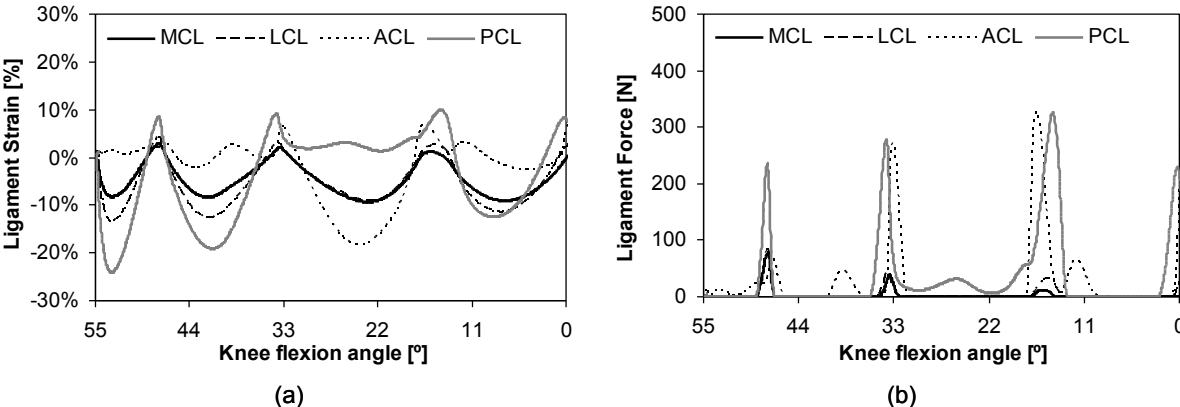
Figure 14. (a) Ligament Strain versus Knee flexion angle for an amplitude of external applied force equal to 150 N; (b) Ligament Force versus Knee flexion angle for an amplitude of external applied force equal to 150 N.
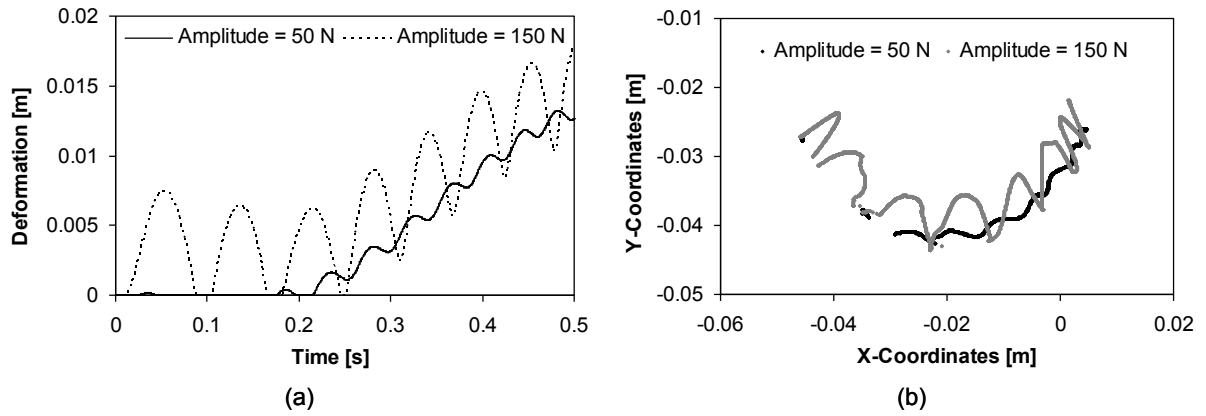
Figure 15. (a) Local deformation/indentation; (b) Tibia contact points.

Since the dynamic response of the ligaments changes with the increase in the amplitude of the external applied force, the deformation is also affected resulting in higher values, as illustrated in Figure 15(a). This difference is due to the fact that the deformation is calculated based on the distance between the femur and the tibia, which is constrained by the ligaments.

A comparative study using two different knee models is performed in what follows. The first model having only ligaments constraints was described and used in all the simulations presented. The second model considers the presence of a clearance and contact between the femur and the tibia. This second model is constructed assuming that the femur acts as a journal and the tibia as a bearing, as illustrated in Figure 16. In what concerns to the geometric configuration, the tibia was considered to be approximately planar, and the femur cartilage was modeled as a curved profile with radius of 0.04 m [54]. The computational simulations take into account the methodology of contact detection presented in Section 3 for the free contact model and the methodology of contact detection described by Flores *et al.* [58] for the clearance revolute joint model. The numerical results obtained are plotted in Figures 17-19.
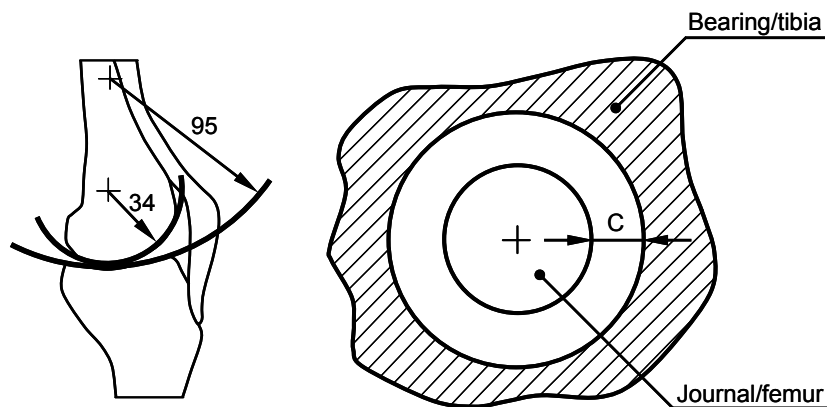

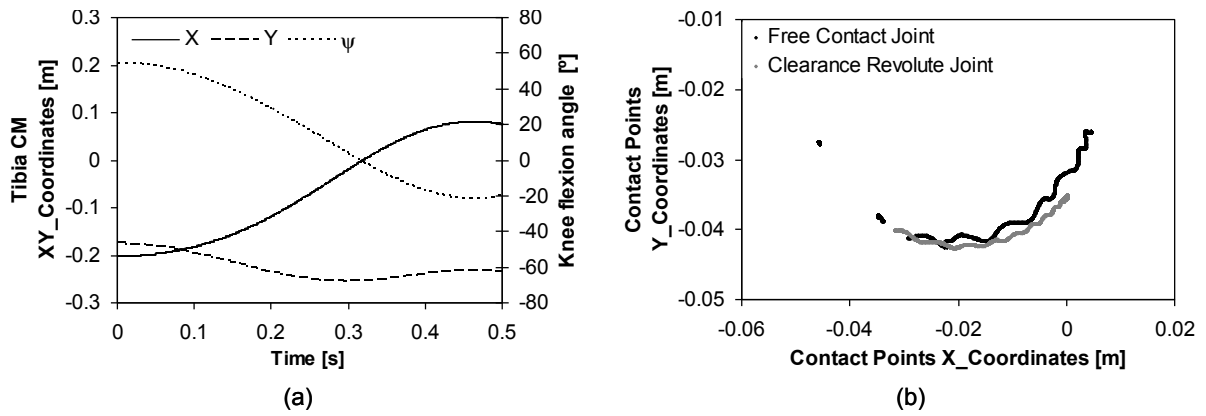Figure 16. Relation between the femur-tibia contact and a revolute clearance joint [58].

Figure 17. (a) Tibia centre of mass coordinates and knee flexion angle for the knee joint modeled as a clearance joint; (b) Tibia contact points for knee joint modeled as free contact joint and as clearance joint.
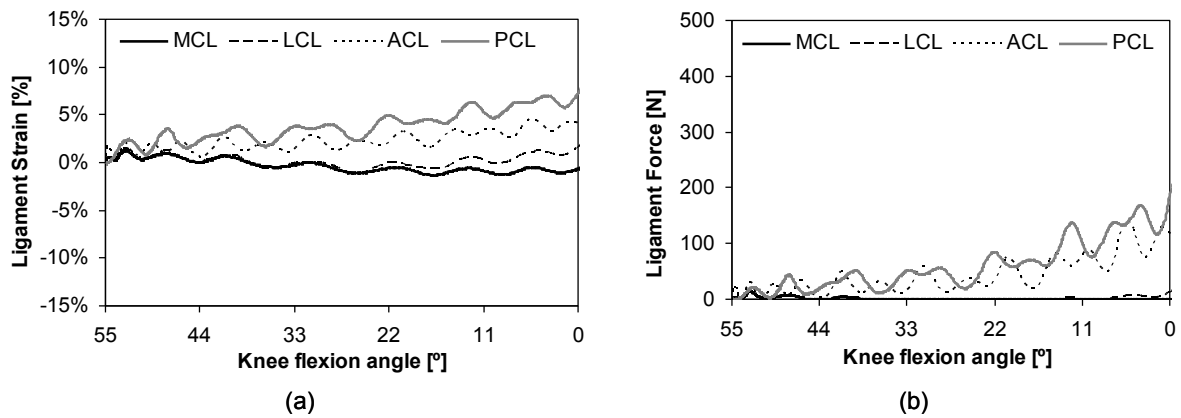

Figure 18. (a) Ligament Strain versus Knee flexion angle for knee joint modeled as clearance joint; (b) Ligament Force versus Knee flexion angle for knee joint modeled as clearance joint.
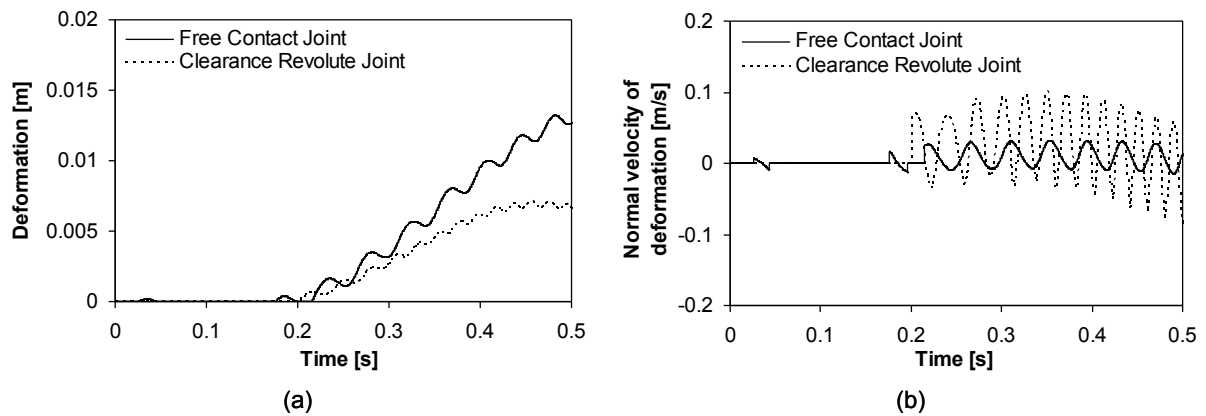

Figure 19. (a) Local deformation/indentation; (b) Normal Velocity of Deformation.

By analyzing Figures 12(a) and 17(a), it can be concluded that the free contact model, for a simulation time equal to 0.5 s, reports a knee flexion angle larger than for the case of the clearance joint model. As the tibia center of mass coordinates are not equivalent for both models, some differences are also reported in the dynamic response of the ligaments, which it is verified by comparing Figures 13 and 18. Since the dynamic response of the ligaments is different in each

model, the results of deformation and normal velocity of deformation diverge, as illustrated Figure 19. This discrepancy occurs because the deformation is calculated based on the distance between the femur and the tibia, which is constrained by the ligaments, and the normal velocity of deformation and the normal contact force depend on the deformation. The same reason explains the differences reported at tibia contact points coordinates plotted in Figure 17(b). The differences between the two models on the knee deformation are related to two facts. First, the knee clearance model is constrained for the ligaments, like the contact free knee model. Secondly, it is constrained by the clearance joint, which is relatively large, since it is considered approximately plane and limits the knee motion. Therefore, the advantage of the free contact modeling in relation to the clearance revolute modeling is that the methodology is more general and can be applied to the analysis of internal contact and external contact between regular or/and complex profiles. This is a great benefit since it offers the possibility to analyze contact between a variety of biological and mechanical systems.

7. Conclusions

A two-dimensional mathematical formulation for the dynamic analysis of the natural human knee joint has been presented in this work. In the process, the main issues related to multibody system formulation were examined and incorporated in a computational algorithm developed to perform dynamic analysis of multibody systems with free contact profiles. The effect the four basic ligaments of the knee namely the cruciate and collateral were incorporated in the model as nonlinear springs. An approach to define the geometry of the contacting outlines based on cubic spline interpolation was proposed. To evaluate the exact location of the contact points between the contacting bodies, a methodology for contact detection has been implemented, which includes three geometric conditions and a penetration condition. A continuous constitutive contact force law was used to evaluate the forces produced during the free contact between the femur and the tibia. The effect of several parameters such as the cubic interpolation spline technique, the elastic contact force model and the amplitude of the external applied force in the knee dynamics was evaluated. The differences on the knee dynamic behavior when this joint was modeled as a free contact joint and as a clearance revolute joint was also studied.

The results obtained indicate that the proposed model is quite sensitive to the procedure utilized to detect contact. The contact force model used has been developed to model impact events between metallic spherical surfaces at high velocities. The biological contact between the cartilages is continuous and present very low velocities. This suggests that a more suitable contact force model to characterize the cartilage dynamic response is required, namely in what concerns the inclusion of joints damping and lubrication effects. Nevertheless, the methodology proposed here

revealed promising perspectives and its general structure allows the prediction of the dynamic response of a healthy human knee joint, as well as knee models that which exhibit some type of pathologies, such as ligament rupture, cartilage defects. Moreover, this proposed formulation can also be useful in the study of the behavior of artificial knees with prosthesis, since this model does not consider the synovial fluid lubricant. The present work can be extended to account for more realistic human joints by developing a three-dimensional model of human knee joint including both 3D surfaces generation and contact detection and force evaluation. In addition, different contact force models can be studied for more "physiological" interactions between the knee parts. The issues related to the lubrication and damping phenomena play a crucial role in this type of multibody system, and therefore will also be target of future research.

Acknowledgments

References

1   Jones, M.L., Hickman, J. and Knox, J. A Validated Finite Element Method Study of Orthodontic Tooth Movement in the Human Subject, *Journal of Orthodontics*, 2001, 28(1) 29-38.

2   Koike, T., Wada, H. and Kobayashi, T. Modeling of the human middle ear using the finite-element method, *Journal of the Acoustical Society of America*, 2002, 111(3) 1306-1317.

3   Halloran, J.P., Petrella, A.J. and Rullkoetter, P.J. A finite element analysis of long stemmed distal tip fixation conditions in tibial knee replacement, *Journal of Biomechanics*, 2006, 39(1), 517-518.

4   Completo, A., Simões, J.A., and Fonseca, F. Explicit finite element modeling of total knee replacement mechanics, *Journal of Biomechanics*, 2005, 38(2), 323-331.

5   Silva, M.P.T. and Ambrósio, J.A.C. Kinematic Data Consistency in the Inverse Dynamic Analysis of Biomechanical Systems, *Multibody System Dynamics*, 2002, 8(2), 219-239.

6   Teng, T-L, Chang, F-A. and Peng, C-P. Analysis of human body response to vibration using multi-body dynamics method, *Proceedings of the Institution of Mechanical Engineers, Part K: Journal of Multi-body Dynamics*, 2006, 220(3), 191-202.

7   van Lopik, D.W. and Acar, M. Analysis of human body response to vibration using multi-body dynamics method, *Proceedings of the Institution of Mechanical Engineers, Part K: Journal of Multi-body Dynamics*, 2007, 221(2), 175-197.

8   van Lopik, D.W. and Acar, M. Dynamic verification of a multi-body computational model of human head and neck for frontal, lateral, and rear impacts, *Proceedings of the Institution of Mechanical Engineers, Part K: Journal of Multi-body Dynamics*, 2007, 221(2), 199-217.

9   Meireles, F., Silva, M., and Flores, P. Kinematic analysis of human locomotion based on experimental data, *Proceedings of the VipImage2007, Thematic Conference on Computational Vision and Medical Image Processing*, Porto, Portugal, October 17-19, 2007, 6p.

10   Raasch, C., Zajac, F., Ma, B. and Levine, S. Muscle Coordination of Maximum-Speed Pedaling, *Journal of Biomechanics,* 1997, 30(6) 595-602.

11   Andriacchi, I. and Hurwitz D. Gait Biomechanics and the Evolution of Total Joint Replacement, *Gait and Posture*, 1997, 5, 256-264.

12   Rasmussen, J., Damsgaard, M., Christensen, S. and Surma, E. Design Optimization with Respect to Ergonomic Properties, *Structural and Mu1tidisciplinan Optimization*, 2002, 24(2), 89-97.

13   Ambrósio, J. and Dias, J. A Road Vehicle Multibody Model for Crash Simulation based on the Plastic Hinges Approach to Structural Deformations, *International Journal of Crashworthiness,* 2007, 12(1), 77-92.

14   Flores, P., Ambrósio, J., Claro, J.C.P., Lankarani, H.M., and Koshy, C.S. Lubricated revolute joints in rigid multibody systems, Nonlinear Dynamics, 2009, 56(3), 277-295.

15   Flores, P., Ambrósio, J., Claro, J.C.P. and Lankarani, H.M. Spatial revolute joints with clearance for dynamic analysis of multibody systems, *Proceedings of the Institution of Mechanical Engineers, Part-K Journal of Multi-body Dynamics*, 2006, 220(4), 257-271.

16   Flores, P., Ambrósio, J., Claro, J.C.P. and Lankarani, H.M. Dynamic behaviour of planar rigid multibody systems including revolute joints with clearance, *Proceedings of the Institution of Mechanical Engineers, Part-K Journal of Multi-body Dynamics*, 2007, 221(2), 161-174.

17   Wismans, J. Veldpaus, F., Janssen, J., Huson, A. and Struben, P. A three-dimensional mathematical model of the knee-joint, *Journal Biomechanics*, 1980, 13(8), 677-685.

18   Hirokawa, S. Biomechanics of the Knee Joint: A Critical Review, *Critical Reviews in Biomedical Engineering*, 1993, 21(2), 79-135.

19   Hawkins, D. and Bey, M. Muscle and tendon force-length properties and their interactions in vivo, *Journal of Biomechanics*, 1997, 30(1), 63-70.

20   Gray, H. *Anatomy of the human body*, Philadelphia, New York: Bartley.com, 2000.

21   Wismans, J. *A three-dimensional mathematical model of the human knee joint*, PhD Dissertation, Eindhoven University of Technology, Eindhoven, The Netherlands, 1980.

22   Moeinzadeh, M.H. T*wo and three-dimensional dynamic modeling of human joint structures with special application to the knee joint*, PhD Dissertation, Ohio State University, Ohio, USA, 1981.

23   Strasser, H. *Lehrbuch der muskel und gelenkmechanik*, Springer, Berlin, Germany, 1917.

24   Menschik, A. Mechanik des kniegelenkes Teil 1, *Z. Orthoped.* 1974, 112, 481.

25   Crowninshield, R., Pope, M.H. and Johnson, R.J. An analytical model of the knee, *Journal of Biomechanics*, 1976, 9, 397-405.

26   Moeinzadeh, M.H., Engin, A.E. and Akkas, N. Two-dimensional dynamic modeling of human knee joint, *Journal of Biomechanics*, 1983, 316(4), 253–264.

27   Abdel-Rahman, E.M. and Hefzy, M.S. A two-dimensional dynamic anatomical model of the human knee joint, *Journal of Biomechanical Engineering* 1993, 115, 357–365.

28   Abdel-Rahman, E.M. and Hefzy, M.S. Three-dimensional dynamic behaviour of the human knee joint under impact loading, *Medical Engineering and Physics*, 1998, 20, 276–290.

29   Engin, A.E. and Tumer, S.T. Improved dynamic model of the human knee joint and its response to impact loading on the lower leg, *Journal of Biomechanical Engineering*, 1993, 115, 137–143.

30   Blankevoort, L. and Huiskes, R. Validation of a three-dimensional model of the knee, *Journal of Biomechanics*, 1996, 29(7), 955–961.

31   Mommersteeg, T.J.A., Blankevoort, L., Huiskes, R., Kooloos, J.G.M., Kauer, J.M.G. and Hendriks, J.C.M. The effect of variable relative insertion orientation of human knee bone–ligament–bone complexes on the tensile stiffness, *Journal of Biomechanics*, 1995, 28(6), 745-752.

32   Piazza, S.J. and Delp, S.L. Three-dimensional dynamic simulation of total knee replacement motion during a step-up task, *Journal of Biomechanical Engineering*, 2001, 123, 599-606.

33   Nikravesh, P.E. *Computer-aided analysis of mechanical systems*, Prentice-Hall, Englewood Cliffs, New Jersey, 1988.

34   Garcia de Jalon, J. and Bayo, E. *Kinematic and Dynamic Simulations of Multibody Systems*, Springer Verlag, New York, 1994.

35   Flores, P. *Dynamic Analysis of Mechanical Systems with Imperfect Kinematic Joints*, PhD Dissertation, University of Minho, Guimarães, Portugal, 2005.

36   Flores, P., Pereira, R., Machado, M., and Seabra, E. Investigation on the Baumgarte Stabilization Method for Dynamic Analysis of Constrained Multibody Systems, Proceedings of EUCOMES08, the

Second European Conference on Mechanism Science Cassino, Italy, (edited by M. Ceccarelli), September 17-19, 2008, Springer, pp. 305-312.

37 Shampine, L. and Gordon, M. C*omputer Solution of Ordinary Differential Equations: The Initial Value Problem*, Freeman, San Francisco, California, 1975.

38 Baumgarte, J. *Stabilization of Constraints and Integrals of Motion in Dynamical Systems*, Computer Methods in Applied Mechanics and Engineering, 1972, 1, 1-16.

39 Marshall, J.L. and Rubin, R.M. Knee ligament injuries - A diagnostic and therapeutic approach, *Orthopedic Clinics of North America*, 1977, 8(3), 641-668.

40 Chapra, S.C. and Canale, R.P. *Numerical Methods for Engineers*, 2nd Edition, McGraw-Hill, 1989.

41 Boor, C. *A practical guide to splines*, Revised Edition, Springer, Berlin, 2001.

42 *IMSL FORTRAN 90 Math Library 4.0. FORTRAN Subroutines for Mathematical Applications*. Visual Numerics, Inc., Houston, USA, 1997.

43 Pombo, J. *A Multibody Methodology for Railway Dynamics Application*. PhD Dissertation, Technical University of Lisbon, Lisbon, Portugal, 2004.

44 Hertz, H. On the contact of solids - On the contact of rigid elastic solids and on hardness. (Translated by D. E. Jones and G. A. Schott), Miscellaneous Papers, Macmillan and Co. Ltd., London, England, 1896, 146-183.

45 Flores, P., Ambrósio, J., Claro, J.C.P., and Lankarani, H.M. Influence of the contact-impact force model on the dynamic response of multibody systems, *Proceedings of the Institution of Mechanical Engineers, Part-K Journal of Multi-body Dynamics*, 2006, 220(1), 21-34.

46 Lankarani, H.M. and Nikravesh, P.E. A Contact Force Model With Hysteresis Damping for Impact Analysis of Multibody Systems, *Journal of Mechanical Design*, 1990, 112, 369-376.

47 Koo, S. and Andriacchi, T.P. A comparison of the influence of global functional loads vs. local contact anatomy on articular cartilage thickness at the knee, *Journal of Biomechanics*, 2007, 40, 2961-2966.

48 Butler, D.L., Grood, E.S., Noyes, F.R. and Zernicke, R.F. Biomechanics of ligaments and tendons, *Exercise and Sports Science Reviews*, 1978, 6, 125-181.

49 Korhonen, R.K., Laasanen, M.S., Töyräs, J., Rieppo, J., Hirvonen, J., Helminen, H.J. and Jurvelin, J.S. Comparison of the equilibrium response of articular cartilage in unconfined compression, confined compression and indentation, *Journal of Biomechanics*, 2002, 35, 903-909.

50 Caplan, A., Elyaderani, M., Mochizuki, Y., Wakitani, S. and Goldberg, V. Overview principles of cartilages repair and regeneration: principles of cartilage repair and regeneration, *Clin. Orthop. Relat. R.*, 1997, 254-269.

51 Petersen, J., Ruecker, A., von Stechow, D., Adamietz, P., Poertner, R., Rueger, J. and Meenen, N. Present and future therapies of articular cartilage defects, *Eur. J. Trauma*, 2003, 1, 1-10.

52 Yamaguchi, G. *Dynamic Moldeling of Musculoskeletal Motiom*. Kluwer Academic Publishers, Dordrecht, The Netherlands, 2001.

53 Li, G., Lopez, O. and Rubash, H. Variability of a three-dimensional finite element model constructed using magnetic resonance images of a knee for joint contact stress analysis, *Journal of Biomechanical Engineering*, 2001, 123, 341-346.

54 Donzelli, P., Spilker, R.S., Ateshian, G.A. and Mow, V.C. Contact analysis of biphasic transversely isotropic cartilage layers and correlation with tissue failure. *Journal of Biomechanics*, 1999, 32, 1037-1047.

55 Tümer, S.T., Engin, A.E., Three-Body Segment Dynamic Model of the Human Knee. Journal of Biomechanical Engineering, 1993, 115, 350-356.

56 Pombo, J., Ambrósio, J.. Application of a wheel-rail contact model to railway dynamics in small radius curved tracks, *Multibody System Dynamics*, 2008, 19, 91-114.

57 Limbert, G., Taylor, M. and Middleton, J. Three-dimensional finite element modelling of the human ACL: simulation of passive knee flexion with a stressed and stress-free ACL, *Journal of Biomechanics*, 2004, 37, 1723-1731.

58 Flores, P., Ambrósio, J., Claro, J.C.P., and Lankarani, H.M. *Kinematics and dynamics of multibody systems with imperfect joints*. Lecture Notes in Applied and Computational Mechanics, 34, Springer-Verlag, Berlin/Heidelberg, Germany, 2008.